Do levels of lipid peroxidation biomarkers reflect the degree of brain injury in newborns?

Mari Merce Cascant-Vilaplana, Ángel Sánchez-Illana, José David Piñeiro-Ramos, Roberto Llorens-Salvador, Guillermo Quintás, Camille Oger, Jean-Marie Galano, Claire Vigor, Thierry Durand, Julia Kuligowski, et al.

News & Views

Do levels of lipid peroxidation biomarkers reflect the degree of brain injury in newborns?

Mari Merce Cascant-Vilaplana[1], Ángel Sánchez-Illana[1], José David Piñeiro-Ramos[1], Roberto Llorens-Salvador[2] Guillermo Quintás[3,4], Camille Oger[5], Jean-Marie Galano[5], Claire Vigor[5], Thierry Durand[5], Julia Kuligowski[1]*, Máximo Vento**[1,6], and the HYPOTOP Study Group

[1]Neonatal Research Group, Health Research Institute Hospital La Fe, Valencia, 46026, Spain

[2]Division of Radiology and Imaging, University & Polytechnic Hospital La Fe, Valencia, 46026, Spain

[3]Health and Biomedicine, Leitat Technological Center, Valencia, 46026, Spain

[4]Unidad Analítica, Health Research Institute La Fe, Valencia, 46026, Spain

[5]Institut des Biomolecules Max Mousseron, UMR 5247 CNRS, ENSCM, Universite de Montpellier, Montpellier, France

[6]Division of Neonatology, University & Polytechnic Hospital La Fe, Valencia, 46026, Spain

*corresponding author; **senior author

Keywords: *Hypoxic-ischemic encephalopathy (HIE); neonatal encephalopathy (NE); newborn; oxidative stress; perinatal asphyxia; lipid peroxidation biomarkers*

Word count: 1901

Number of references: 9

Number figures: color figures: 2 (online 2 and print 0)

Abstract

The pathogenesis and progression of Hypoxic-Ischemic Encephalopathy (HIE), a major cause of severe neurological disability and mortality in the perinatal period, is shaped by the interplay of multiple processes including inflammation, oxidative stress, and excitotoxicity. We conducted a longitudinal study determining biomarkers of oxidative stress and inflammation in non-invasive urine samples of newborns with moderate/severe HIE (N=51) employing Liquid Chromatography - Mass Spectrometry. We noted that levels of several biomarkers of oxidative stress increased over time demonstrating the ongoing propagation of oxidative injury. Prostaglandins, in contrast, showed a decreasing trend in their concentration profiles over time, which probably reflects their mediation on pathogenic mechanisms, including the inflammatory response. Statistically significant differences in the levels oxidative stress of neonates with distinct brain lesion patterns, as detected with Magnetic Resonance Imaging (MRI), were observed, revealing an increase of lipid peroxidation biomarkers in newborns with cerebral lesions (MRI score 1) as compared to scores 0 and 2. Moreover, a gender-dependent study showed no statistically significant differences in biomarker concentrations between male and female infants. Our observation leads to the hypothesis that the monitoring of non-invasive lipid peroxidation biomarkers could aid diagnosis and predicting of long-term outcomes as complementary tool to standard explorations.

Graphical Abstract: Figure 1.

Introduction

Approximately 10% of newborns require assistance to initiate breathing at birth, and around 2% require resuscitation with clinical and/or biochemical signs of perinatal asphyxia with ca. 20% of these infants developing hypoxic ischemic encephalopathy (HIE), a major cause of severe neurological disability and perinatal mortality. Strong evidence indicates that the pathogenesis and progress ion of HIE is shaped by the interplay of multiple processes including inflammation, oxidative stress, and excitotoxicity which finally lead to brain injury. After a hypoxic-ischemic insult, brain cells initially undergo impaired oxidative metabolism, followed by reperfusion injury that leads to the death of neuronal cells. Neuronal death is triggered by a cascade of events which include reactive oxygen species (ROS). The generation of ROS is involved in physiological reactions during the fetal-to-neonatal transition, and it has been demonstrated that ROS generation up-regulates the expression of specific genes whose end-products are beneficial for postnatal adaptation. However, triggered by hypoxia and ischemia, ROS production rapidly increases and overwhelms antioxidant defenses and ultimately lead to the development of specific conditions. Hence, the beneficial and toxic effects of O_2 administration for newborn therapy need to balance to prevent cellular and tissue damage. Both, hypoxia and reoxygenation, generate excessive amounts of ROS and subsequently, oxidative stress. Several studies illustrate molecular and metabolomics changes associated with asphyxia, duration of hypoxia, and resuscitation with different oxygen concentrations. At high concentrations, ROS modify or degenerate a range of macromolecules, such as lipids, proteins, and polysaccharides and can damage DNA and RNA and lead to a cascading inflammatory response. The neonatal brain with a high concentration of polyunsaturated fatty acids (PUFAs), high rate of oxygen consumption, low concentration of antioxidants, and high levels of iron is especially vulnerable to excessive amounts of ROS. Inflammation is considered as an important contributor in the pathophysiology of cerebral HI injury. The initial inflammatory response to HI produces a secondary neuronal injury followed by an anti-inflammatory response toward resolution of inflammation.

The state-of-the-art reference method for the early characterization of structural damage of the grey matter (i.e., the basal ganglia, the thalamus, and the cortex) and to a lesser extent infarction in white matter, is magnetic resonance imaging (MRI) acquired within 5-7

days after birth. The prognostic ability of MRI obtained in the neonatal period to determine neurodevelopmental outcomes in childhood has been demonstrated (8). Currently, literature providing evidence of the relationship between oxidative stress biomarkers and the degree of brain damage is scant and based on the comparison of HIE versus healthy control infants and determinations in blood samples. In preterm infants, a reference range for lipid peroxidation byproducts in urine samples was established and preterm babies who later developed bronchopulmonary dysplasia (BPD), a disease associated to oxidative stress, showed significantly higher urinary elimination of isofurans in analytical determinations performed during the first days after birth (5).

Access to an early and accurate, biomarker-guided diagnosis of neonatal HIE could be a powerful ally to reduce neonatal mortality, morbidity, and degree of disability, through a personalized adjustment of treatment options. In the present study, we monitored urinary oxidative biomarkers levels in a cohort of term newborns with moderate or severe HIE before, during, and after TH. We compared oxidative stress levels between neonates with different degrees of brain injury vs. normal MRI outcomes following a standardized scoring system (8) and carried out a gender-dependent study of the detected oxidative stress biomarkers.

Results

A sub-cohort of 51 newborns from the HYPOTOP trial recruiting infants with moderate or severe HIE qualifying for TH were included in this study. Relevant clinical and demographic characteristics are summarized in Table 1. A total of 22 patients (43%) had normal (score 0) and 29 (57%) pathologic (scores 1, 2 or 3) MRI outcomes. There was no statistically significant difference among both groups (i.e., normal and pathologic MRI outcomes) regarding gestational age (GA), gender, and biometric characteristics (Table 1). From this population, 24 (47%) patients were males and 27 (53%) females and there was no statistically significant difference between recorded clinical parameters between genders.

A total of 234 urine samples were collected before the initiation of TH (N=28) and at 12 (N=37), 24 (N=41), 48 (N=47), 72 (N=42), and 96 hours (N=39) after the initiation of TH. Serial collection of urine samples enabled the longitudinal assessment of the evolution of urinary oxidative stress biomarkers before and during cooling and upon rewarming. Out of measured lipid peroxidation compounds, five resolved isoprostanoids and six total

intensities of relative UPLC-MS/MS signals characteristic of lipid peroxidation products (i.e., total parameters) were detected (i.e., levels above the Limit of Quantification, LOQ) in 50% of samples. Two out of five measured prostaglandins (PGs) were detected, in addition to one biomarker of oxidative damage to DNA and one out of four biomarkers of oxidative damage to proteins. Median values and IQR of each determined parameter, as well as the detection frequency are shown in Table 2. No significant trend in the levels of 5(*RS*)-5-F $_{2t}$-IsoP, 15(*RS*)-15-F_{2t}-IsoP, 2,3-dinor-15-F_{2t}-IsoP, 4(*RS*)-4-F_{4t}-NeuroP as well as total IsoPs, IsoFs, NeuroPs, NeuroFs and dihomo-IsoFs was observed during the study period. However, levels of 14(*RS*)-14-F_{4t}-NeuroP, 6-keto-$PGF_{1\alpha}$, $PGF_{2\alpha}$, sum of 7-series dihomo-IsoPs, mTyr/Phe, and 8OhdG/2dG presented significant changes compared to the initial levels (Figure 2A). The levels of biomarkers of oxidative stress including isoprostanoids and biomarkers of damage to DNA and proteins, increased over time, while PG levels decreased.

Urinary biomarker levels of 5(*RS*)-5-F_{2t}-IsoP, 2,3-dinor-15-F_{2t}-IsoP, 15(*RS*)-15-F_{2t}-IsoP, 4(*RS*)-4-F_{4t}-NeuroP, 14(*RS*)-14-F_{4t}-NeuroP, 6-keto-$PGF_{1\alpha}$, $PGF_{2\alpha}$, as well as total IsoPs, IsoFs, NeuroPs, NeuroFs, dihomo-IsoPs, dihomo-IsoFs, mTyr/Phe, and 8OhdG/2dG were compared between infants with MRI scores 0 (no injury), 1 (1A: minimal and 1B: extensive cerebral lesions), and 2 (2A: basal ganglia thalamic, anterior or posterior limb of internal capsule and watershed infarction and 2B: 2A with cerebral lesions) (8). Only two infants of this cohort had severe brain injury (score 3), and hence, this subgroup was excluded from statistical analysis. Thus, three binary partial least squares discriminant analysis (PLSDA) models were built to assess metabolic differences between patients with MRI scores 0, 1 and 2. Receiver operating characteristic (ROC) curves based on the results obtained by leave-one-patient-out cross validation were calculated (Figure 2B, top). Biomarker levels found in infants with MRI score 1 were significantly different from the other two groups (i.e., MRI scores 0 and 2) as confirmed by permutation testing (p-values ≤0.003), while no statistically significant difference was found between MRI scores 0 and 2. *Variable* Importance in Projection (VIP) scores vs. regression vector (Figure 2B, bottom) were used to measure the influence of each metabolite on the PLSDA models. Several determined biomarkers showed characteristic patterns in samples from newborns belonging to the MRI score 1 group, i.e., levels of 14(*RS*)-14-F_{4t}-NeuroP, total IsoPs, 15(*RS*)-

15-F_{2t}-IsoP, and total dihomo-IsoPs were higher in infants with MRI score 1 than score 0 or score 2 (Figure 2B bottom, left and middle).

Finally, levels of oxidative stress biomarkers in male vs. female infants were assessed in the search of sex-specific associations. However, no statistically significant differences were found (data not shown).

Discussion

This is the first study to examine the relationship between a large panel of oxidative stress and inflammatory biomarkers and brain injury in infants with moderate/severe HIE. Our data demonstrate that specific indicators for oxidative stress mediated damage and inflammation can be longitudinally monitored in newborns with HIE, thanks to the use of non-invasively collected urine samples. The results (Figure 2A) reflect an increase of a specific NeuroP isomer (i.e., 14(*RS*)-14-F $_{4t}$-NeuroP) as well as total dihomo-IsoPs over the study period revealing protracted oxidative stress that persisted during TH and the rewarming period. NeuroPs are lipid mediators generated by non-enzymatic lipid peroxidation of docosahexaenoic acid (DHA), a polyunsaturated fatty acid highly abundant in brain tissue and have been suggested as markers of oxidative damage to brain tissue, urine, plasma, or cerebrospinal fluid (9). Dihomo-IsoPs, derived from radical attack on adrenic acid (AdA), are considered biomarkers of cerebral white matter injury. Likewise, increasing levels of biomarkers of damage to proteins (mTyr/Phe) and DNA (8OhdG/2dG) were observed. The spontaneous oxidation of Phe in presence of hydroxyl free radicals produces m-Tyr and o-Tyr that are stable molecules, and their concentrations are useful markers of oxidative protein damage. Protein oxidation has been associated with neuronal dysfunction in vivo and may be involved in the pathology of neurodegenerative disorders (1). 8OHdG, produced by the oxidation of the nucleotide 2dG, is excreted in urine and is commonly used as biomarker of oxidative damage to DNA (7). Oxidative stress is strongly related to acute brain damage in children, and 8-OHdG is a useful marker of brain damage (3).

Simultaneously we studied inflammatory biomarkers in HIE. Decreasing levels of biomarkers of PGs (i.e., 6-keto-PGF $_{1\alpha}$ and PGF $_{2\alpha}$) were observed. PGs are produced by the enzymatic peroxidation of AA, and they play a key role in the inflammatory response. Inflammation is a response to injury, and it is an intrinsically beneficial event that leads to

removal of offending factors and restoration of tissue structure and physiological function. PGs, particularly prostaglandins E and F_2, lead to cerebral vasodilation and their concentrations increase in response to cerebral ischemia (4). More specifically, 6-keto-$PGF_{1\alpha}$, a stable metabolite of prostacyclin also known as prostaglandin I_2 (PGI_2), is a vasodilative and is associated with brain perfusion and cerebral infarction. It is probably the most important PG due to its effect on sensory neurons (2). The decrease of PGs with time observed in the present study might reflect a progressive return to normal levels after the hypoxic insult that occurred before/during delivery.

Access to biomarkers that early and accurately diagnose oxidative stress and response could potentially aid the diagnosis and improve prognosis of newborns with HIE. In this regard, we compared between infants with pathologic and normal MRI outcomes by using standardized scores discerning between injury patterns. Our data provides evidence of oxidative stress biomarker changes in urine samples of newborns with HIE depending on their lesion type. Specifically, biomarker patterns in urine samples from newborns with MRI score 1 were significantly different from scores 0 and 2, while no difference between the latter sub-groups were found. Infants belonging to the sub-groups with MRI score 0 and 2 presented lower values of DHA-derived NeuroPs (14(*RS*)-14-F_{4t}-NeuroP), AA-derived IsoPs (total IsoPs and 15(*RS*)-15-F_{2t}-IsoP), and AdA-derived dihomo-IsoPs (total dihomo-IsoPs) in comparison to infants with MRI score 1. Thus, lipid peroxidation biomarker profiles linked to oxidative damage of different PUFAs, which are all highly abundant in the brain, change according to specific injury patterns (i.e., MRI score 1).

Previous studies established male sex as a risk factor for unfavorable outcome of HIE during the perinatal period regardless of lesion types. Some authors found notable differences between microglia and neuroimmune signaling in the male and female brain and suggested that these differences play a relevant role . However, in this study we did not observe consistent and significant alterations between male and female infants associated to oxidative stress levels.

In summary, this is the first study presenting detailed insights on the evolution of a broad panel of oxidative stress and inflammation biomarkers in newborns infants with moderate/severe HIE undergoing TH. We identified a set of biomarkers with constantly increasing concentrations that demonstrate the propagation of oxidative injury through

the whole study period including the secondary phase of HIE. PGs, in contrast, showed a decreasing tendency which reflects inflammatory response. We found statistically significant differences in newborns with different patterns of pathologic vs. normal HIE outcomes, but not between male and female infants.

Innovation

Oxidative stress and inflammation are known to be deeply involved in the pathogenesis of cerebral lesions in newborns after a hypoxic-ischemic insult. However, the determination of specific related biomarkers for diagnosis and prediction of long-term outcomes as a complementary tool to standard evaluations is not yet exploited in newborn critical care. Our findings demonstrate the feasibility and potential usefulness of a continuous monitoring of biomarkers in non-invasive biofluids from newborn infants with HIE undergoing therapeutic hypothermia as oxidative stress and inflammation biomarkers may provide clinically relevant additional information on the patient's status and progression.

Notes

Study approval and population

The study was approved by the Ethics Committee for Biomedical Research of the Health Research Institute La Fe (Valencia, Spain) and registered under the acronym HYPOTOP (EudraCT 2011-005696-17). The HYPOTOP trial is a randomized, controlled, multicenter, double-blinded clinical trial for assessing the efficacy of topiramate *vs* placebo in newborns with HIE undergoing TH. All methods were performed in accordance with relevant guidelines and regulations and informed consent was obtained from legal representatives of enrolled infants. For a detailed description of the HYPOTOP trial, including the study design and the established inclusion and exclusion criteria, the reader is referred to the literature (6). In this study, a sub-cohort of 51 newborns enrolled in the HYPOTOP trial was included.

Samples were collected following a standard operating procedure to avoid bias, systematic errors, and flaws related to the experimental design. Urine samples were collected before initiation of TH (within 6h of delivery) and at 12, 24, 48, 72, and 96 h after the initiation of TH. Urine samples were aliquoted into dry microcentrifuge tubes and stored immediately at -80 :C until analysis.

Magnetic Resonance Imaging

MRI was carried out using different high-field magnet systems between days 4 and 8 after birth. 3D Gradient Echo T1 weighted MR images, axial Fast Spin Echo T2 weighted MR images, and diffusion weighted images were acquired. The interpretation of MRI results was carried out by an experienced, blinded pediatric neuroradiologist rating the extent of the injury in posterior limb internal capsule, basal ganglia, and thalamus, white matter, and cortex and using a standardized score according to the National Institute of Child Health and Human Development (NICHD) Neonatal Research Network (NRN), discerning between injury patterns as described by Shankaran et al. (8).

Standards and reagents

LC-MS grade solvents (methanol CH_3OH, ethanol, heptane and acetonitrile CH_3CN) were purchased from J.T. Baker (Phillipsburg, NJ, USA). Formic acid (HCOOH, 98%) and ethyl acetate (analytical grade) were from Panreac (Barcelona, Spain). Ultrapure H_2O was generated on a milliQ system from Merck Millipore (Darmstadt, Germany).

For lipid biomarker determinations, commercially available IsoPs (2,3-dinor-15-F_{2t}-IsoP CAS No. 221664-05-7) (16290), 15-keto-15-E_{2t}-IsoP (Item No. 14390; CAS No. 914804-63-0) (14390), 15-keto-15-F_{2t}-IsoP (CAS No. 191919-01-4) (16390), 15-E_{2t}-IsoP (CAS No. 27415-25-4) (14350, 15-F_{2t}-IsoP) (CAS No. 27415-26-5) (16350), PGs (PGE_2 (CAS No. 363-24-6) (14010), $PGF_{2\alpha}$ (CAS No. 551-11-1) (16010), 11β-$PGF_{2\alpha}$ (CAS No. 38432-87-0) (16520), 6-keto-$PGF_{1\alpha}$ (CAS No. 58962-34-8) (15210), and dihomo-PG (1α,1β-dihomo-$PGF_{2\alpha}$ (CAS No. 57944-39-5) (16050)) were purchased from Cayman Chemical Company (Ann Arbor, MI, USA), with purities ≥95% as well as deuterated internal standards (IS) (PGF $_{2\alpha}$-D_4 (CAS No. 34210-11-2) (316010), 10-*epi*-10-F_{4t}-NeuroP-D_4, and 15-F_{2t}-IsoP-D_4 (CAS No. 211105-40-7) (316350)) with purities ≥98% and ≥99% incorporation of deuterated form (D_1-D_4) and <1% D_0. Other analytical standards employed were F $_2$-IsoPs (5(*RS*)-5-F $_{2t}$-IsoP), F $_4$-NeuroPs (4(*RS*)-4-F_{4t}-NeuroP, 10-*epi*-10-F_{4t}-NeuroP, 10-F_{4t}-NeuroP, 14(*RS*)-14-F_{4t}-NeuroP), F_4-NeuroF (4(*RS*)-ST-Δ^5-8-NeuroF), F_2-dihomo-IsoPs (17-F_{2t}-dihomo-IsoP, *ent*-7(*RS*)-7-F_{2t}-dihomo-IsoP), and F_2-dihomo-IsoFs (17(*RS*)-10-*epi*-SC Δ^{15}-11-dihomo-IsoF, 7(*RS*)-ST-Δ^8-11-dihomo-IsoF) synthesized at the *Institut des Biomolecules Max Mosseron* (Montpellier, France) with purities ≥99% and all physical data reported in those published articles confirming their structures.

Standards of o-Tyr (CAS No 2370-61-8) (93851), m-Tyr (CAS No.775-06-4) (T3629), Phe (CAS No. 63-91-2) (78019), $3NO_2$-Tyr (CAS No. 621-44-3) (N7389) 3Cl-Tyr (CAS No. 7423-93-0) (512443), p-Tyr (CAS No. 556-03-6) (145726), 8OHdG (CAS No. 88847-89-6) (H5653), and 2dG (CAS No. 312693-72-4) (D-7145)) (>96% w/w purity) were obtained from Sigma-Aldrich (St. Louis, MO, USA). The ISs Tyr-D_2 (CAS No. 30811-19-9) (DLM-449-1), 2dG-$^{13}C^{15}N_2$ (CNLM-6836-SL) and 8OHdG-$^{13}C^{15}N_2$ were purchased from Cambridge Isotope Laboratories and Phe-d_5 from CDN Isotopes (Pointe-Claire, Canada).

Isoprostanoid determination

10 µL of β-glucuronidase solution (10 mg mL^{-1}) were added to 600 µL of urine samples previously thawed on ice and homogenized and were incubated at 37 ^{o}C during 90 min. After incubation,

300 µL of IS solution (100 nM) in H_2O (0.1% v/v HCOOH, pH 3):CH_3OH (85:15 v/v) was added, homogenized, and centrifuged at 16000 g for 10 min at 4 ^{o}C. For clean-up and preconcentration, solid-phase extraction (SPE) using Discovery®DSC-18 SPE 96-well plates (Sigma-Aldrich) was carried out. SPE cartridges were conditioned with 1 mL of CH_3OH followed by rinsing with 1 mL of H_2O (0.3% v/v HCOOH, pH 3):CH_3OH (95:5 v/v). The diluted samples were loaded onto the SPE plate followed by washing with 500 µL of H_2O and 500 µL of heptane. Cartridges were dried with room air and sample extracts were eluted with 4 x 100 µL ethyl acetate which were subsequently evaporated using a miVac centrifugal vacuum concentrator from Genevac LTD (Ipswich, UK). Sample extracts were dissolved in 60 µL of H_2O (0.1% v/v HCOOH, pH 3):CH_3OH (85:15 v/v) prior to Ultra Performance Liquid Chromatography coupled to tandem Mass Spectrometry (UPLCMS/MS) analysis.

Samples were analyzed using an Acquity-Xevo TQS system from Waters (Milford, MA) operating in negative electrospray ionization (ESI-) mode using a Waters BEH C18 reversed-phase column (2.1 x 100 mm, 1.7 µm) and a binary H_2O (0.1% v/v formic acid):CH_3CN (0.1% v/v formic acid) gradient.

The UPLC-MS/MS method was based on our previous validated methods for the quantification of lipid peroxidation biomarkers (7). The measurement parameters used for the studied biomarkers are summarized in Table 2. Biomarker concentrations were normalized to creatinine. To quantify creatinine concentration, a Urinary Creatinine

Detection Kit (Arbor Assays™, Ann Arbor, MI, USA) was employed. A dilution of 1:4 (v/v) of samples with H_2O and a 96 well plate microreader (Halo LED 96, Dynamica Scientific Ltd., Newport Pagnell, UK) were used, measuring the absorbance at 490 nm.

Biomarkers of proteins and DNA oxidation

The determination of biomarkers of oxidative damage to DNA and proteins was performed following a previously validated UPLC-MS/MS method (7). 50 µL of IS solution (1 µM) in H_2O (0.1% v/v HCOOH) were added to 50 µL of centrifuged urine sample. For UPLC-MS/MS analysis, samples were loaded on 96-well plates and analysed randomly using an Acquity-Xevo TQ system from Waters operating in the positive electrospray ionization (ESI+) mode. Separations were performed using an Acquity UPLC BEH C18 reversed-phase column (2.1 · 50 mm, 1.7 µm) from Waters and a CH_3OH (0.05% v/v formic acid): H_2O (0.05% v/v formic acid) binary gradient. Parameters used for the measurement of different metabolites are summarized in Table 2. For comparisons between samples, the following metabolite ratios were determined: m-Tyr/Phe, o-Tyr/Phe, 3Cl-Tyr/pTyr, $3NO_2$-Tyr/pTyr and 8OHdG/2dG.

Statistical analysis

UPLC-MS/MS data were acquired and processed using MassLynx 4.1 and QuanLynx 4.1 (Waters, Milford, MA), respectively. Values below the LOQ were replaced by ½ LOQ. Further data analysis was carried out in MATLAB R2019b (Mathworks Inc., Natick, MA, USA) using in-built as well as in-house written scripts and functions and the PLS Toolbox 8.0 (Eigenvector Research Inc., Wenatchee, USA). Partial least squares discriminant analysis (PLSDA) of autoscaled data and leave-one-patient-out cross validation were build. Receiver operating characteristic (ROC) curves were based on PLSDA models. Significance of models was tested by permutation testing (500 permutations). Group comparisons of demographic and clinical characteristics were carried out by using the Student's t-test for unequal variances, Chi square test or Wilcoxon ranksum test for parametric, categorical and non-parametric variables, respectively. *P*-values<0.05 were considered as statistically significant.

Acknowledgments

The authors express their gratitude to the parents and their newborns who participated in the study. Technical assistance of the *Servicio de Soporte a la Investigación Experimental* (SCSIE) at the University of Valencia (Spain) is acknowledged.

Members of the HYPOTOP Study Group: Isabel Izquierdo, Ana Gimeno, María Gormaz, Raquel Escrig, María Cernada, Marta Aguar, Ester Torres (Division of Neonatology, University and Polytechnic Hospital La Fe, Valencia, Spain); Isabel Benavente-Fernández (Division of Neonatology, University Hospital Puerta del Mar, Cádiz, Spain); Eva Valverde, Malaika Cordeiro (Division of Neonatology, University Hospital La Paz, Madrid, Spain); Dorotea Blanco (Division of Neonatology, University Hospital Gregorio Marañón, Madrid, Spain); Hector Boix (Department of Neonatology, University Hospital Vall d'Hebrón, Barcelona, Spain); Fernando Cabañas (Division of Neonatology, University Hospital Quirónsalud Madrid, Madrid, Spain); Mercedes Chaffanel (Division of Neonatology, Regional University Hospital Málaga, Málaga, Spain); Belén Fernández-Colomer (Division of Neonatology, Central University Hospital of Asturias, Oviedo, Spain); Jose Ramón Fernández-Lorenzo (Division of Neonatology, University Hospital Complex of Vigo, Vigo, Spain); Begoña Loureiro (Division of Neonatology, University Hospital Cruces, Bilbao, Spain); Maria Teresa Moral-Pumarega (Division of Neonatology, University Hospital 12 de Octubre, Madrid, Spain); Antonio Pavón (Division of Neonatology, University Hospital Virgen del Rocío, Sevilla, Spain); and Inés Tofé (Division of Neonatology, University Hospital Reina Sofía, Córdoba, Spain).

Authorship confirmation statement

All authors have made substantial contributions to the conception or design of the work, or the acquisition, analysis, or interpretation of data for the work. All authors were involved in the drafting of the work or its critical revision for important intellectual content. All authors gave their final approval of the version to be published. All authors agreed to be accountable for all aspects of the work in ensuring that questions related to the accuracy or integrity of any part of the work are appropriately investigated and resolved.

Authors' disclosure statement

The authors declare no conflict of interest.

Funding statement

This research was funded by *Instituto de Salud Carlos III* [grant numbers CP16/00034, CD19/00037, PI17/00127, and PI20/00964].

Abbreviations

AdA: adrenic acid

ESI^+: positive electrospray ionization

ESI^-: negative electrospray ionization

GA: gestational age

HIE: Hypoxic ischemic encephalopathy

IsoFs: isofuranoids

IsoPs: isoprostanoids

LOQ: limit of quantification

MRI: magnetic resonance imaging

m-Tyr: meta-tyrosine

NeuroFs: neurofuranoids

NeuroPs: neuroprostanoids

o-Tyr: ortho-tyrosine

PGs: prostaglandins

Phe: phenylalanine

p-Tyr: para-tyrosine

PUFAs: polyunsaturated fatty acids

ROS: reactive oxygen species

SPE: solid-phase extraction

TH: therapeutic hypothermia

UPLC-MS/MS: ultra-performance liquid chromatography–tandem mass spectrometry

References

1. Butterfield D. Brain protein oxidation in age-related neurodegenerative disorders that are associated with aggregated proteins. *Mech Ageing Dev* 122: 945–962, 2001.
2. Dray A. Inflammatory mediators of pain. *Br J Anaesth* 75: 125–131, 1995.
3. Fukuda M, Yamauchi H, Yamamoto H, Aminaka M, Murakami H, Kamiyama N, Miyamoto Y, and Koitabashi Y. The evaluation of oxidative DNA damage in children with brain damage using 8-hydroxydeoxyguanosine levels. *Brain Dev* 30: 131–136, 2008.
4. Inder TE and Volpe JJ. Pathophysiology. In: *Volpe's Neurology of the Newborn*. Elsevier, 2018, pp. 325-388.e26.
5. Kuligowski J, Aguar M, Rook D, Lliso I, Torres-Cuevas I, Escobar J, Quintas G, Brugada M, Sanchez-Illana A, van Goudoever JB, and Vento M. Urinary lipid peroxidation byproducts: are they relevant for predicting neonatal morbidity in preterm infants? *Antioxid Redox Signal*, 2015.
6. Nuñez-Ramiro A, Benavente-Fernández I, Valverde E, Cordeiro M, Blanco D, Boix H, Cabañas F, Chaffanel M, Fernández-Colomer B, Fernández-Lorenzo JR, Kuligowski J, Loureiro B, Moral-Pumarega MT, Pavón A, Sánchez-Illana A, Tofé I, Hervás D, García-Robles A, Parra-Llorca A, Cernada M, Martinez-Rodilla J, Lorente-Pozo S, Llorens R, Marqués R, Vento M, and on behalf of the Hypotop Study Group. Topiramate plus Cooling for Hypoxic-Ischemic Encephalopathy: A Randomized, Controlled, Multicenter, Double-Blinded Trial. *Neonatology* 116: 76–84, 2019.
7. Parra-Llorca A, Gormaz M, Sánchez-Illana Á, Piñeiro-Ramos JD, Collado MC, Serna E, Cernada M, Nuñez-Ramiro A, Ramón-Beltrán A, Oger C, Galano J-M, Vigor C, Durand T, Kuligowski J, and Vento M. Does Pasteurized Donor Human Milk Efficiently Protect Preterm Infants Against Oxidative Stress? *Antioxid Redox Signal* 31: 791–799, 2019.
8. Shankaran S, McDonald SA, Laptook AR, Hintz SR, Barnes PD, Das A, Pappas A, Higgins RD, and Eunice Kennedy Shriver National Institute of Child Health and Human Development Neonatal Research Network. Neonatal Magnetic Resonance Imaging Pattern of Brain Injury as a Biomarker of Childhood Outcomes following a Trial of Hypothermia for Neonatal Hypoxic-Ischemic Encephalopathy. *J Pediatr* 167: 987-993.e3, 2015.

9. Signorini C, De Felice C, Durand T, Galano J-M, Oger C, Leoncini S, Ciccoli L, Carone M, Ulivelli M, Manna C, Cortelazzo A, Lee JC-Y, and Hayek J. Relevance of 4-F4t-neuroprostane and 10-F4t-neuroprostane to neurological diseases. *Free Radic Biol Med* 115: 278–287, 2018.

Correspondence Address

*corresponding author: Julia Kuligowski; Neonatal Research Group, Health Research Institute La Fe, Avenida Fernando Abril Martorell 106, 46026 Valencia, Spain; julia.kuligowski@uv.es

**senior author: Máximo Vento; Division of Neonatology, University & Polytechnic Hospital La Fe & Neonatal Research Group, Health Research Institute La Fe, Avenida Fernando Abril Martorell 106, 46026 Valencia, Spain; maximo.vento@uv.es

Figure legends

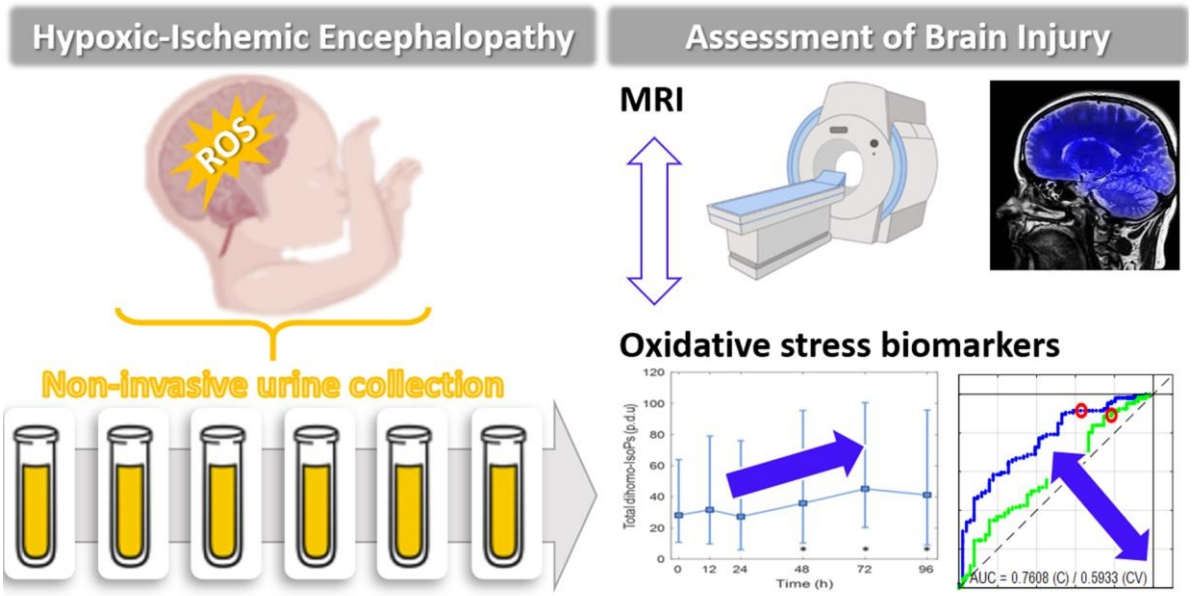

Figure 1. The study of noninvasive urine samples provides allows a longitudinal monitoring of newborn infants with Hypoxic-Ischemic Encephalopathy (HIE) undergoing therapeutic hypothermia treatment. The determination of oxidative stress biomarkers such as biomarkers of oxidative damage to lipids by Liquid Chromatography coupled to tandem Mass Spectrometry might provide clinically relevant information complementary to routine evaluations such as Magnetic Resonance Imaging of the brain.

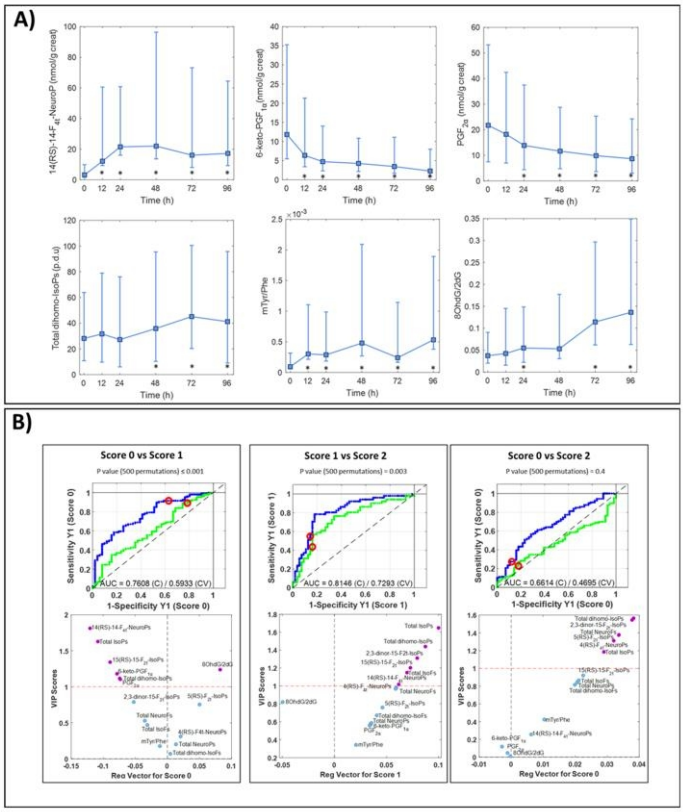

Figure 2. (A) Longitudinal evolution of biomarker levels detected in urine samples from newborns with HIE that present significant changes over time with respect to initial levels (*p-values<0.05, Wilcoxon rank-sum test, α=0.05). Values below LOQ were replaced by ½ x LOQ. Data were expressed as median and inter-quartile range (IQR 25% - 75%). **(B)** Biomarker profiles found in urine samples from newborns with HIE and different MRI scores. ROC curves (top) and VIP scores vs. regression vectors (bottom) from PLSDA discerning between MRI scores 0 vs. 1 (left), 1 vs. 2 (middle), and 0 vs. 2 (right). Note: blue lines represent estimated PLSDA ROC curves (calibration set); green lines represent estimated PLSDA ROC curves (cross validation); dashed lines represent 50% lines; and circles indicate model thresholds.

Table1. Clinical and demographic data of newborns included in the study

	Moderate /Severe HIE (N=51)	**Normal MRI (N=22)**	**Pathologic MRI (N=29)**	**p-value**	**male (N=24)**	**female (N=27)**	**p-value**
Gestational age (weeks) median (IQR)	39 (38-40)	38 (37-40)	39 (38-40)	0.5	38 (37-40)	39 (38-40)	0.7
Gender (male), n (%)	24 (47%)	11 (50%)	13 (45%)	0.7	24 (100%)	0 (0%)	<0.001
Weight (g) mean ± SD	3265 ± 639	3321 ± 566	3222 ± 696	0.6	3400 ± 629	3400 ± 635	0.16
Lenght (cm) mean ± SD	51 ± 3	52 ± 4	50 ± 3	0.2	52 ± 3	52 ± 4	0.09
Head circumfere	34.4 ± 1.8	35 ± 1.5	34 ± 2	0.5	35.0 ± 1.5	35.0 ± 1.8	0.04

nce (cm) mean ± SD							
TPM treatment, n (%)	21 (41%)	9 (41%)	15 (52%)	0.4	14 (58%)	10 (37%)	0.13
Sarnat 2 / Sarnat 3	36/15	17/5	19/10	0.4	14/10	22/3	0.07
MRI (normal), n (%)	22 (43%)	22 (100%)	0 (0%)	<0.001	11 (46%)	11 (41%)	0.7
MRI score[a] (%)							
Score 0	22 (43%)	22 (100%)	0 (0%)	<0.001	11 (46%)	10 (37%)	0.5
Score 1	9 (18%)	0 (0%)	9 (33%)	0.002	5 (21%)	5 (19%)	0.8
Score 2	14 (27%)	0 (0%)	14 (48%)	<0.001	8 (33%)	6 (22%)	0.37
Score 3	2 (4%)	0 (0%)	2 (7%)	0.2	0 (0%)	2 (7%)	0.200
Apgar	2 (1-3)	2 (1-4)	1 (1-3)	0.5	1 (0-3)	2 (1-3)	0.0

1min, median (IQR)							207
Apgar 5min, median (IQR)	4 (2-5)	4 (3-5)	3 (1-5)	0.16	3 (1-4)	5 (2-5)	0.06
Apgar 10min, median (IQR)	5 (4-8)	5 (4-8)	5 (4-6)	0.3	4 (3-5)	6 (4-7)	0.02

Data were expressed as mean ± SD (standard deviation) for parametric variables, number of cases (percentages) for categorical variables and median (inter-quartile range, IQR 0.25% - 0.75%) for non-parametric variables. To compare between the two groups, Students t-test, Chi square test or Wilcoxon ranksum test (α=0.05), were employed, respectively. For four newborns no information on the degree of injury was available.

Table2. Acquisition parameters and main figures of merit of the LC-MSMS methods

Oxidative damage	Analyte	m/z Parent ions	Cone [V]	CE [eV]	m/z Daughter ions	RT ± s (min)		Calibration range (nM)		R^2	Internal Standard	median (nM)	IQR		>LOQ (%)
Lipid peroxidation	5(*RS*)-F_{2t}-IsoP	353.2	35	30	115	4.270	± 0.010	0.7	- 2338	0.997	$PGF_{2\alpha}$-d_4	16	7	- 38	100
	2,3-dinor-15-F_{2t}-IsoP	325.27	40	13	237	3.061	± 0.003	0.7	- 2338	0.996	15-F_{2t}-IsoP-d_4	42	26	- 70	100
	15(*RS*)-15-F_{2t}-IsoP	353	35	30	193	4.003	± 0.002	1.4	- 2338	0.998	15-F_{2t}-IsoP-d_4	10	5	- 16	87
	15-keto-15-F_{2t}-IsoP	351	35	25	289	4.282	± 0.009	5.5	- 2339	0.993	$PGF_{2\alpha}$-d_4	—		– –	16
	15-E_{2t}-IsoP + PGE_2	351	35	30	271	4.552	± 0.003	5.5	- 1169	0.998	$PGF_{2\alpha}$-d_4	—		– –	0.4
	15-keto-15-E_{2t}-IsoP	349	40	30	113	4.7	± 0.0	0.7	- 29	0.9	$PGF_{2\alpha}$-d_4	—		–	11

																22
					9	0		2	9			–				
					2	8			7							
					4.	0.			0.							
	37				8	0	0.	2	9							
4(*RS*)-F_{4t}-	7.	2	1	271	2	±	7	-	9	PGF$_{2\alpha}$			-			96
NeuroP	32	0	9	.12	6	1	1	2	5	-d_4	4	2	8			
					4.	0.		1	0.							
	37				3	0	0.	1	9							
10-*epi*-10-F_{4t}-	7.	1	1	153	3	±	7	-	9	PGF$_{2\alpha}$			–			0
NeuroP	32	0	9		0	0		6	5	-d_4	—		–			
					4.	0.		2	0.	15-						
	37				1	0	0.	9	9	F_{2t}-						
10-F_{4t}-NeuroP	7.	1	1	153	9	±	7	-	9	IsoP-			–			0
	32	0	9		2	2		2	8	d_4	—		–			
					4.	0.		2	0.							
	37				4	0	1.	3	9	PGF$_{2\alpha}$						
14(*RS*)-14-F_{4t}-	7.	5	1	204	7	±	4	-	9	-d_4			-			93
NeuroP	32	0	9	.89	8	0		3	8		23	7	52			
					4.	0.		2	0.							
	39				9	0	4	3	9							
4(*RS*)-ST-Δ^5-8-	3.	4	3	123	4	±	3.	-	3	PGF$_{2\alpha}$						0
NeuroF	6	0	5	.19	8	0	8		8	-d_4	—		–			
					5.	0.		1	0.							
	38				0	0	0.	1	9	PGF$_{2\alpha}$						
17(*RS*)-F_{2t}-	1.	2	2	337	2	±	7	-	9	-d_4			–			0
dihomo-IsoP	3	0	5	.15	6	1		6	2		—		–			
					5.	0.		2	0.							
	38				0	0	0.	3	9	PGF$_{2\alpha}$						
ent-7(*RS*)-F_{2t}-	1.	5	2	142	2	±	7	-	9	-d_4			–			0
dihomo-IsoP	3	0	5	.98	3	0		3	8		—		–			

17(*RS*)-10-*epi*-SC-Δ^{15}-11-dihomo-IsoF	397.4	20	31	155.02	5.47 ± 4.49	0.01	0.7	-16.99	0.90	$PGF_{2\alpha}$-d_4	—	–	–		0
7(*RS*)-ST-Δ^{8}-11-dihomo-IsoF	397.4	40	25	201.03	4.99 ± 3.93	0.00	1.4	-16.99	0.97	$PGF_{2\alpha}$-d_4	—	–	–		0
1α,1β-dihomo $PGF_{2\alpha}$	381.3	20	25	337.15	5.42 ± 4.23	0.00	0.7	-17.3	0.98	15-F_{2t}-IsoP-d_4	—	–	–		0
11ß-$PGF_{2\alpha}$	353	35	30	193	4.13 ± 5.38	0.00	0.7	-16.99	0.98	15-F_{2t}-IsoP-d_4	—	–	–		0
6-keto-$PGF_{1\alpha}$	369	40	35	245	3.27 ± 5.75	0.00	0.7	-23.38	0.98	15-F_{2t}-IsoP-d_4	6	3	- 13		93
$PGF_{2\alpha}$	353	35	30	193	4.42 ± 8.34	0.01	0.7	-16.99	0.98	$PGF_{2\alpha}$-d_4	17	9	- 29		99
15-F_{2t}-IsoP-d_4	357	40	30	197	4.02 ± 1.99	0.00	—	—	—		—	–	–		100
$PGF_{2\alpha}$-d_4	357	40	30	197	4.44 ± 4.99	0.00	—	—	—		—	–	–		100

						15	09					-		
	Total IsoPs	353.2	35	30	115	—	—	—	$PGF_{2\alpha}$-d_4	91	54	-	164	100
	Total IsoFs	369.2	45	20	115	—	—	—	$PGF_{2\alpha}$-d_4	114	67	-	198	100
	Total NeuroPs	377	35	20	101	—	—	—	$PGF_{2\alpha}$-d_4	1086	656	-	2143	100
	Total NeuroFs	393	35	20	193	—	—	—	$PGF_{2\alpha}$-d_4	63	41	-	108	100
	Total dihomo-IsoPs	381	20	20	143	—	—	—	$PGF_{2\alpha}$-d_4	46	32	-	66	100
	Total dihomo-IsoFs	397	35	25	155	—	—	—	$PGF_{2\alpha}$-d_4	4	2	-	8	100
Protein oxidation	oTyr	182.1	30	15	136.1	2.187 ± 0.005	11 – 1136	0.997	Phe-d_5	–		–		11
	mTyr	182.1	30	15	136.1	1.478 ± 0.008	4 – 284	0.998	pTyr-d_2	4	4	-	18	56
	pTyr	182.1	30	15	136.1	1.141 ± 0.007	360 – 227272	0.990	pTyr-d_2	26814	1356 7	-	5374 7	100
	3ClTyr	216.1	25	15	170.1	2.882 ± 0.006	4 – 2273	0.999	Phe-d_5	–		–		19

	$3NO_2Tyr$	227.1	25	15	168.1	3.178 ± 0.006	4 – 1136	0.990	Phe-d_5	–		–		16
	Phe	166.1	25	15	120.1	2.708 ± 0.018	90 - 227272	0.995	Phe-d_5	20048	1055	-	3819	100
	Phe-d_5	171.1	35	10	125	2.646 ± 0.012	–	–	–	–		–		100
	pTyr-d_2	184.1	15	20	138.09	1.133 ± 0.009	–	–	–	–		–		100
DNA oxidation	8OHdG	284.1	20	15	168.1	3.131 ± 0.007	1 – 284	0.992	8OHdG$^{13}C^{15}N_2$	4	2	-	8	89
	2dG	268	15	10	152	1.999 ± 0.019	1 - 1136	0.997	2dG$^{13}C^{15}N_2$	60	29	-	137	100
	8OHdG$^{13}C^{15}N_2$	287	25	10	171	3.137 ± 0.012	–	–	–	–		–		100
	2dG$^{13}C^{15}N_2$	271	15	10	155.1	1.989 ± 0.013	–	–	–	–		–		100

CE: collision energy; RT: retention time; Median and interquartile range (IQR) of detected analytes in urine samples